Neurochem Res (2012) 37:223–231
DOI 10.1007/s11064-011-0597-9

ORIGINAL PAPER

Combination Effects of Sodium Butyrate and Pyridoxine Treatment on Cell Proliferation and Neuroblast Differentiation in the Dentate Gyrus of D-Galactose-Induced Aging Model Mice

Dae Young Yoo · Woosuk Kim · In Hye Kim · Sung Min Nam · Jin Young Chung · Jung Hoon Choi · Yeo Sung Yoon · Moo-Ho Won · In Koo Hwang

Received: 31 August 2011 / Accepted: 8 September 2011 / Published online: 5 October 2011

Abstract We previously reported that sodium butyrate (SB), a histone deacetylase inhibitor, robustly increased pyridoxine-induced cell proliferation and neuroblast differentiation in the dentate gyrus of the adult mouse. In this study, we investigated the effects of treatment with SB combined with pyridoxine on cell proliferation and neuroblast differentiation in the dentate gyrus of a mouse model of aging induced by D-galactose (D-gal). D-gal was administered to 20-week-old male mice (D-gal mice) for 10 weeks to induce changes that resemble natural aging in animals. Seven weeks after D-gal (100 mg/kg) treatment, vehicle (physiological saline; D-gal-vehicle mice) and SB (300 mg/kg) combined with pyridoxine (Pyr; 350 mg/kg) were administered to the mice (D-gal-Pyr-SB mice) for 3 weeks. Escape latency under water maze in the D-gal mice was longer than that in the control mice. In the D-gal-Pyr-SB mice, escape latency was similar to that in the control mice. In the D-gal mice, many cells in the granule cell layer of the dentate gyrus showed pyknosis and condensation of the cytoplasm. However, in the D-gal-Pyr-SB mice, such cellular changes were rarely found. Furthermore, the D-gal mice showed a great reduction in cell proliferation (Ki67-positive cells) and neuroblast differentiation (doublecortin-positive neuroblasts) in the dentate gyrus compared to control mice. However, in the D-gal-Pyr-SB mice, cell proliferation and neuroblast differentiation were markedly increased in the dentate gyrus. Furthermore, the administration of pyridoxine with sodium butyrate significantly increased Ser133-phosphorylated cyclic AMP response element binding protein in the dentate gyrus. These results indicate that the combination treatment of Pyr with SB in D-gal mice ameliorated the D-gal-induced reduction in cell proliferation, neuroblast differentiation, and memory deficits.

Keywords Hippocampus · Aging · Neurogenesis · Histone deacetylase inhibitor · Memory deficit · Vitamin B_6 · Ki67 · Doublecortin

D. Y. Yoo · W. Kim · S. M. Nam · Y. S. Yoon · I. K. Hwang (✉)
Department of Anatomy and Cell Biology, College of Veterinary Medicine, and Research Institute for Veterinary Science, Seoul National University, Seoul 151-742, South Korea
e-mail: vetmed2@snu.ac.kr

I. H. Kim
Department of Physiology, College of Medicine, Hallym University, Chuncheon 200-702, South Korea

J. Y. Chung
Department of Neurology, Seoul National University Hospital, Seoul 110-744, South Korea

J. H. Choi
Department of Anatomy, College of Veterinary Medicine, Kangwon National University, Chuncheon 200-701, South Korea

M.-H. Won (✉)
Department of Neurobiology, School of Medicine, Kangwon National University, Chuncheon 200-701, South Korea
e-mail: mhwon@kangwon.ac.kr

Introduction

The hippocampus is an important brain region that plays a central role in memory. Recently, it has been suggested that newly generated cells from the subgranular zone that migrate to the granule cell layer of the dentate gyrus might be involved in aspects of normal hippocampal function, such as spatial learning and memory [1–3]. Neurogenesis declines dramatically in the dentate gyrus in the aged brain, and this is closely related to cognitive decline [4–9].

D-galactose (D-gal) is a naturally occurring substance in the body, and many studies have demonstrated that reactive oxygen species can be generated during the course of D-gal metabolism [10–13]. Chronic administration of D-gal induces age-related phenotypes, such as cognitive dysfunction [14–16], neurodegeneration [17–20], and the formation of advanced glycation endproducts [12, 21].

Neurogenesis involves the birth, differentiation, maturation, migration, and survival of newly generated neurons. Many factors influence neurogenesis in the dentate gyrus. Changes in chromatin structure due to posttranslational modifications of histones are associated with a number of behavioral events, including memory formation [22–24]. In addition, histone protein modifications, such as acetylation and deacetylation, play a key role in regulating gene expression during the processes of cell proliferation and differentiation [25].

In a previous study, we observed that pyridoxine (Pyr, vitamin B_6) significantly increased cell proliferation and neuroblast differentiation in the mouse dentate gyrus without any neuronal damage [26]. In addition, we found that sodium butyrate (SB), a histone deacetylase (HDAC) inhibitor, robustly increased Pyr-induced cell proliferation and neuroblast differentiation in the mouse dentate gyrus [27]. In the present study, we investigated whether the stimulation of neurogenesis in the brain might yield benefits for cerebral dysfunctions that are associated with the aging induced by D-gal.

Experimental Procedures

Experimental Animals

Male C57BL/6 mice were purchased from Japan SLC Inc. (Shizuoka, Japan). They were housed in a conventional state under adequate temperature (23°C) and humidity (60%) control with a 12 h light/12 h dark cycle, and could freely access food and tap water. The handling and the care of the animals conformed to the guidelines established in order to comply with current international laws and policies (NIH Guide for the Care and Use of Laboratory Animals, NIH Publication No. 85-23, 1985, revised 1996), and were approved by the Institutional Animal Care and Use Committee (IACUC) of Seoul National University (SNU-100628-6). All of the experiments were conducted with an effort to minimize the number of animals used and the suffering caused by the procedures used in the present study.

Drug Treatment

The animals were divided into 2 groups: control ($n = 13$) and 100 mg/kg D-gal ($n = 26$, Sigma, St. Louis, MO)-treated group. The latter group was further classified into 2 subgroups ($n = 13$ in each subgroup): 1) vehicle (physiological saline)-treated (D-gal-vehicle) group, and 2) 350 mg/kg Pyr combined with 300 mg/kg SB (Sigma, St. Louis, MO)-treated (D-gal-Pyr-SB) group. D-gal was subcutaneously administered to 20-week-old mice once a day for 10 weeks. At 7 weeks after D-gal administration, vehicle or Pyr was intraperitoneally administered to mice twice a day for 3 weeks, and SB was subcutaneously treated to mice at the same age once a day for 3 weeks. These schedules were adopted because doublecortin (DCX, a marker for neuroblasts) is exclusively expressed in immature neurons from 1 to 28 days of cell age [28, 29].

Water Maze Performance

At the 10th week after D-gal administration, spatial memory was assayed with Morris water maze. At 3 days after the training, the time required for individual mouse to find the submerged platform within 2 min (escape latency) and the swimming distance were monitored by a digital camera and a computer system for 4 consecutive days and 4 trials per day. The administration of D-gal, SB and Pyr was continued during the water maze performance.

Tissue Processing

For histology, control, D-gal-vehicle, and D-gal-Pyr-SB groups ($n = 8$ in each group) at the day after water maze test were anesthetized with 30 mg/kg Zoletil 50 (Virbac, Carros, France) and perfused transcardially with 0.1 M phosphate-buffered saline (PBS, pH 7.4), which was followed by 4% paraformaldehyde in 0.1 M phosphate-buffer (PB, pH 7.4). Brains were removed and postfixed in the same fixative for 4 h. For hematoxylin and eosin staining (H&E) and phosphorylated cyclic AMP response element at Ser133 (pCREB) immunohistochemistry, the brain tissues ($n = 3$) were dehydrated with graded concentrations of alcohol for embedding in paraffin. Three-μm-thick sections were serially cut using a microtome (Leica), and they were mounted onto silane-coated slides. The sections were stained with H&E staining according to the general protocol. For immunohistochemical staining, the brain tissues ($n = 5$) were cryoprotected by infiltration with 30% sucrose overnight. The 30-μm-thick brain sections were serially cut in the coronal plane using a cryostat (Leica, Wetzlar, Germany). The sections were collected in six-well plates containing PBS until further processing.

Immunohistochemistry

In order to obtain accurate data for immunohistochemistry, free-floating sections were carefully processed under the

same conditions. The tissue sections were selected between −1.46 mm and −2.46 mm posterior to the bregma in reference to a mouse atlas [30] for each animal. Ten sections were in 90 μm apart from each other, and the sections were sequentially treated with 0.3% hydrogen peroxide (H_2O_2) in PBS and 10% normal goat or rabbit serum in 0.05 M PBS. For pCREB immunohistochemistry, the sections were placed in 400 ml jars filled with citrate buffer (pH 6.0) and heated in a microwave oven (Optiquick Compact, Moulinex) operating at a frequency of 2.45 GHz and 800 W power setting. After three heating cycles of 5 min each, slides were allowed to cool at room temperature and washed in PBS. They were next incubated with diluted rabbit anti-Ki67 (a marker for cell proliferation) antibody (1:1,000; Abcam, Cambridge, UK), goat anti-DCX antibody (1:50; Santa Cruz Biotechnology, Santa Cruz), or rabbit anti-pCREB (diluted 1:1,000, Millipore, Temecula, CA) overnight, and subsequently exposed to biotinylated rabbit anti-goat, or goat anti-rabbit IgG (diluted 1:200; Vector, Burlingame, CA) and streptavidin peroxidase complex (diluted 1:200, Vector). Then, the sections were visualized by reaction with 3,3'-diaminobenzidine tetrahydrochloride (Sigma).

The measurement of Ki67-, DCX-, and pCREB-positive cells in all the groups was performed using an image analysis system equipped with a computer-based CCD camera (software: Optimas 6.5, CyberMetrics, Scottsdale, AZ). In addition, images of all DCX-immunoreactive structures were taken from the dentate gyrus through a BX51 light microscope (Olympus, Tokyo, Japan) equipped with a digital camera (DP71, Olympus) connected to a computer monitor. The dendritic complexity of DCX-positive cells was traced using camera lucida at 100 × magnification (Neurolucida; MicroBrightField, Williston, VT). DCX-positive cells were separated into 2 categories according to dendritic complexity. The first category contained cells that lacked dendrites or had immature dendrites with primary or secondary branches which did not extend into the outer molecular layer. The second category contained cells that had mature dendrites with tertiary branches which extended into the outer molecular layer. Then, the DCX-positive cells in each section of the dentate gyrus were counted using Optimas 6.5 software (CyberMetrics). The cell counts from all of the sections of all of the mice were averaged.

Western Blot Analysis

To confirm the effects of SB combined with Pyr on neuroblast differentiation, the dentate gyrus were dissected out using PixCell II system (Arcturus Engineering). The tissues were homogenized in 20 mM PBS (pH 7.4) containing 0.1 mM ethylene glycol bis (2-aminoethyl Ether)-N,N,N',N' tetraacetic acid (EGTA) (pH 8.0), 0.2% Nonidet P-40, 10 mM ethylendiamine tetraacetic acid (EDTA) (pH 8.0), 15 mM sodium pyrophosphate, 100 mM β-glycerophosphate, 50 mM NaF, 150 mM NaCl, 2 mM sodium orthovanadate, 1 mM phenylmethylsulfonyl fluoride (PMSF) and 1 mM dithiothreitol (DTT). After centrifugation, the protein level was determined in the supernatants using a Micro BCA protein assay kit with bovine serum albumin as the standard (Pierce Chemical, Rockford, IL). Aliquots containing 20 μg of total protein were boiled in loading buffer containing 150 mM Tris (pH 6.8), 3 mM DTT, 6% SDS, 0.3% bromophenol blue and 30% glycerol. The aliquots were then loaded onto a polyacrylamide gel. After electrophoresis, the gels were transferred to nitrocellulose transfer membranes (Pall Corp., East Hills, NY). To reduce background staining, the membranes were incubated with 5% non-fat dry milk in PBS containing 0.1% Tween 20 for 45 min, followed by incubation with goat anti-DCX (1:100), peroxidase-conjugated anti-goat IgG (Sigma) and an enhanced luminol-based chemiluminescent (ECL) kit (Pierce Chemical). The blot was densitometrically scanned for the quantification of relative optical density of each band using Scion Image software (Scion Corp., Frederick, MD). These data were normalized against β-actin.

Statistical Analysis

The data presented represent the means of the experiments performed for each experimental investigation. The differences among the means were statistically analyzed by a one-way analysis of variance followed by a Tukey's multiple range method in order to elucidate differences among groups.

Results

Spatial Memory

None of the mice tested showed any obvious health problems, such as weight loss or toxic reactions. The escape latency in the D-gal-vehicle group was longer than that in the control group for all days (Fig. 1). In the D-gal-Pyr-SB group, the escape latency was significantly decreased compared to that in the D-gal-vehicle group, and it was similar to that in the control group for all days (Fig. 1).

Hematoxylin & Eosin (H&E) Staining

In the control group, round granule cells were easily observed in the dentate gyrus (Fig. 2a). In the D-gal-vehicle

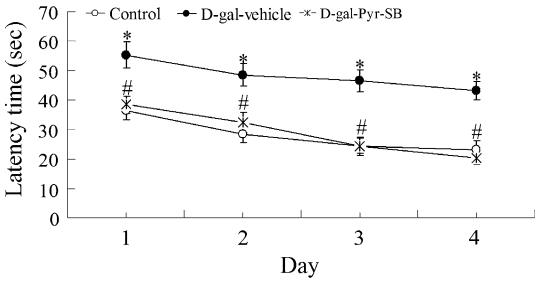

Fig. 1 Spatial memory test using a Morris water maze in the control, D-gal-vehicle, and D-gal-Pyr-SB groups ($n = 17$ per group; $^{*}P < 0.05$, indicating a significant difference compared to the control group; $^{\#}P < 0.05$, significantly different from the D-gal-vehicle group). *Bars* indicate standard errors (SE)

group, many cells that were located in the subgranular zone of the dentate gyrus showed pyknosis and condensed cytoplasm (Fig. 2b). In the D-gal-Pyr-SB group, the H&E staining pattern was similar to that in the control group (Fig. 2c).

Cell Proliferation

In the control group, Ki67-positive nuclei were mainly detected in the subgranular zone of the dentate gyrus (Fig. 3a). These nuclei were clustered, and the mean number was 10.4 per section (Fig. 3d). In the D-gal-vehicle group, Ki67-positive nuclei were significantly decreased compared to that in the control group, and the mean number of Ki67-positive nuclei was 6.5 per section (Fig. 3b, d). In the D-gal-Pyr-SB group, Ki67-positive nuclei were robustly increased in the dentate gyrus compared to that in the D-gal-vehicle group, and the number of Ki67-positive nuclei was similar to that in the control group. The mean number of Ki67-positive nuclei was 10.7 per section (Fig. 3c, d).

Neuroblast Differentiation

In the control group, doublecortin (DCX)-immunoreactive neuroblasts were detected in the subgranular zone of the dentate gyrus, and many of them had tertiary dendrites that extended into the upper two-thirds of the molecular layer of the dentate gyrus (Fig. 4a, b). In this group, the mean number of DCX-immunoreactive neuroblasts with and without tertiary dendrites was 9.4 and 14.2 per section, respectively, in the dentate gyrus (Fig. 4g). In the D-gal-vehicle group, DCX-immunoreactive neuroblasts were markedly decreased in the dentate gyrus compared to the control group, and only a few DCX-immunoreactive neuroblasts had tertiary dendrites (Fig. 4c, d). In this group, the mean number of DCX-immunoreactive

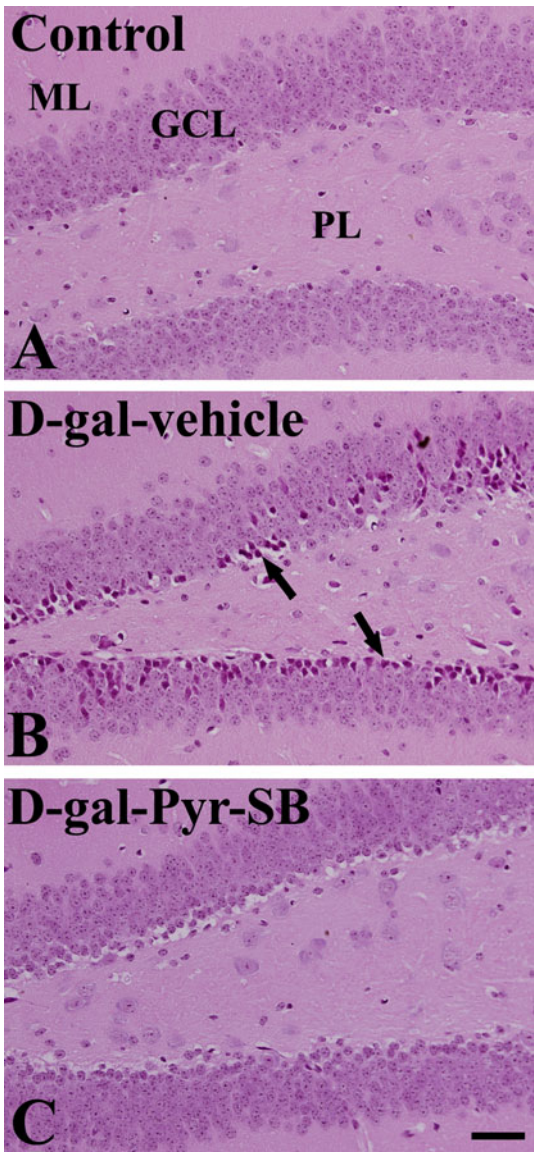

Fig. 2 Hematoxylin & Eosin (H&E) staining in the dentate gyrus of the control (**a**), D-gal-vehicle (**b**), and D-gal-Pyr-SB (**c**) groups. Pyknosis and cytoplasmic condensation (*arrows*) are observed in the subgranular layer of the D-gal-vehicle group. In the D-gal-Pyr-SB group, overall morphology is similar to that in the control group. *GCL* granule cell layer, *ML* molecular layer, *PL* polymorphic layer. *Scale bar* = 50 μm

neuroblasts with and without tertiary dendrites was 2.4 and 8.3 per section, respectively, in the dentate gyrus (Fig. 4g). In the D-gal-Pyr-SB group, the dendrites of DCX-immunoreactive neuroblasts were much more complex compared to the D-gal-vehicle group (Fig. 4e, f). In the D-gal-Pyr-SB group, the mean number of DCX-immunoreactive neuroblasts with and without tertiary dendrites was 38.2 and 56.3 per section, respectively, in the dentate gyrus (Fig. 4g).

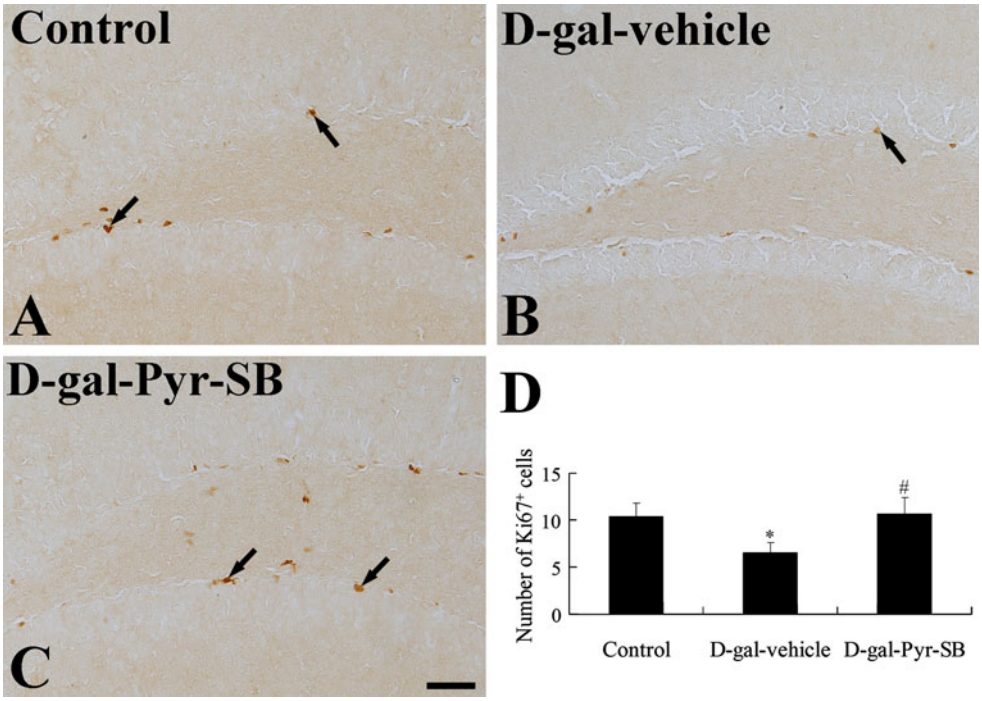

Fig. 3 Immunohistochemistry for Ki67 in the dentate gyrus of the control (**a**), D-gal-vehicle (**b**), and D-gal-Pyr-SB (**c**) groups. Ki67-positive cells (*arrows*) are observed in the dentate gyrus. Ki67-positive nuclei are markedly decreased in the D-gal-vehicle group. In the D-gal-Pyr-SB group, the number of Ki67-positive nuclei is similar to that in the control group. *GCL* granule cell layer, *ML* molecular layer, *PL* polymorphic layer. *Scale bar* = 50 μm. **d** The mean number of Ki67-positive cells per section in all groups ($n = 7$ per group; $^{*}P < 0.05$, indicating a significant difference compared to the control group; $^{\#}P < 0.05$, significantly different from the D-gal-vehicle group). The *bars* indicate the SE of the mean (SEM)

DCX Protein Levels

DCX protein levels were markedly decreased in the D-gal-vehicle group compared to that in the control group. In this group, the relative percentage of the protein levels was 57.6% of the control group. However, in the D-gal-Pyr-SB group, DCX protein levels were much higher than that in the D-gal-vehicle group, and the relative percentage of the protein levels was 835.2% of the D-gal-vehicle group (Fig. 5).

pCREB Immunohistochemistry

In the control group, pCREB-positive nuclei were observed in the subgranular zone of the dentate gyrus (Fig. 6a). In the D-gal-vehicle group, pCREB-positive nuclei were significantly decreased: only a few pCREB-positive nuclei were observed in the subgranular zone (Fig. 6b). In this group, the mean percentage of the pCREB-positive nuclei was 43.6% of the control group (Fig. 6d). In the D-gal-Pyr-SB group, pCREB-positive nuclei were distinctively increased (Fig. 6c), and the mean percentage of the pCREB-positive nuclei was 330.6% of the D-gal-vehicle group (Fig. 6d).

Discussion

The D-gal-induced acceleration of senescence has been used for brain aging studies because the D-gal-induced behavioral and neurochemical changes in the brain can mimic many characteristics of the aging process in humans [15, 21, 31]. In the present study, the administration of D-gal significantly impaired cognitive performance and caused severe neuronal damage in the mouse dentate gyrus. These deficits were restored by the treatment of Pyr combined with SB. This result is supported by previous studies that mice treated with D-gal showed cognitive deficits [13, 17, 32]. In addition, it was reported that D-gal significantly increased deoxynucleotidyl-transferase-mediated UTP nick-end-labeled cells in the dentate gyrus [17, 20]. In a mouse model of Alzheimer's disease, chronic injections of HDAC inhibitors, such as sodium valproate, sodium butyrate, or vorinostat, completely restored contextual memory [33]. In a normative aging study, higher concentrations of vitamin B-6 were related to better performance in memory in aged humans [34].

The administration of D-gal for 10 weeks in the present study significantly reduced cell proliferation and neuroblast differentiation in the dentate gyrus. This result is supported by a previous study that showed that the number of proliferating progenitor cells in the mouse dentate gyrus was significantly decreased the 7th week after D-gal administration [17], and they reported that the surviving number of newly born cells in the dentate gyrus of D-gal-treated mice was significantly decreased in comparison with controls [17]. In addition, the

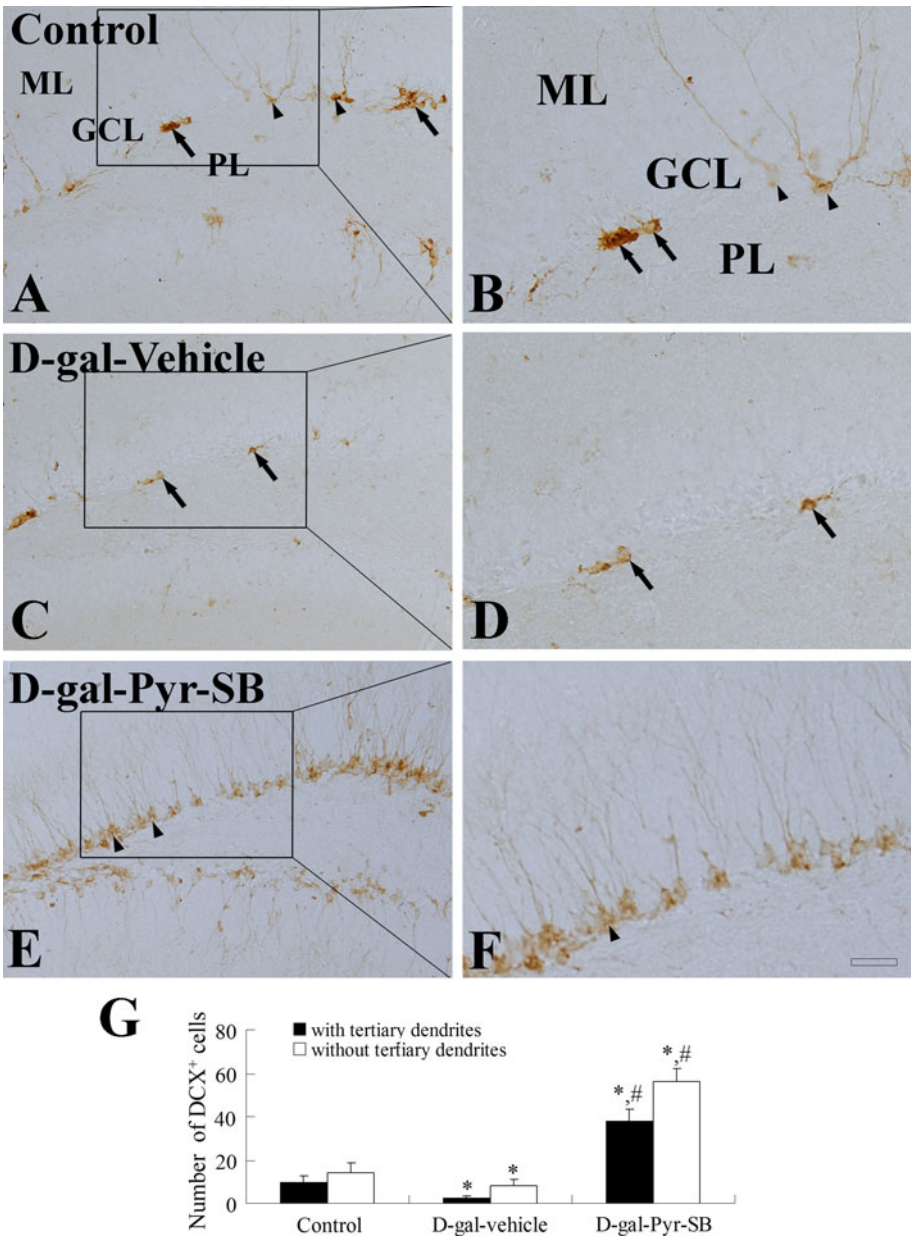

Fig. 4 Immunohistochemistry for doublecortin (DCX) in the dentate gyrus of the control (**a**, **b**), D-gal-vehicle (**c**, **d**), and D-gal-Pyr-SB (**e**, **f**) groups. In the control group, DCX-immunoreactive neuroblasts with (*arrowheads*) and without (*arrows*) tertiary dendrites are easily observed. In the D-gal-vehicle group, DCX-immunoreactive neuroblasts are distinctively decreased compared to the control group. DCX-immunoreactive neuroblasts in the D-gal-Pyr-SB group are much more abundant than in the control group. *GCL* granule cell layer, *ML* molecular layerm, *PL* polymorphic layer. *Scale bar* = 50 μm (**a**, **c**, and **e**) or 25 μm (**b**, **d**, and **f**). **g** The mean number of DCX-immunoreactive neuroblasts with and without tertiary dendrites per section in all the groups ($n = 7$ per group; $^{*}P < 0.05$, indicating a significant difference compared to the control group; $^{\#}P < 0.05$, significantly different from the D-gal-vehicle group). The *bars* indicate the SEM

impairment in hippocampal neurogenesis was similar to that in normally aging mice [7, 35].

The administration of Pyr combined with SB significantly ameliorated the D-gal-induced reduction of cell proliferation and neuroblast differentiation in the dentate gyrus. The oral administration of Pyr is easily absorbed in the intestine and converted into its active forms, such as pyridoxamine and pyridoxal phosphate, which act as coenzymes in the biosynthesis of GABA, dopamine, and serotonin [36]. In our previous study, we observed that the administration of Pyr significantly increased cell proliferation and neuroblast differentiation in the dentate gyrus by upregulating GABA levels without any neuronal damage [26]. In addition, deficits of vitamin B_6 in utero significantly reduced the number of total neurons and normal neurons in the neocortex with an increase in the number of shrunken neurons (700–1,500% of controls) [37].

In contrast, an artificial inhibition of HDACs increased the acetylation and transcription of some genes and enhanced hippocampal-dependent memory formation [38–40]. In the present study, we used SB to inhibit HDAC activity in the dentate gyrus. We previously found that treatment of Pyr combined with SB in D-gal-

administered adult mice significantly increased cell proliferation and neuroblast differentiation in the dentate gyrus [27].

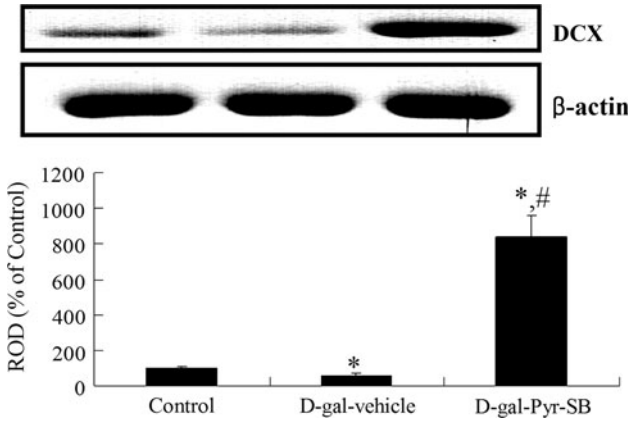

Fig. 5 Western blot analysis of DCX in the dentate gyrus from the control, D-gal-vehicle, and D-gal-Pyr-SB groups. The relative optical density (ROD) of immunoblot bands is represented as % values ($n = 5$ per group; $^{*}P < 0.05$, indicating a significant difference compared to the control group; $^{\#}P < 0.05$, significantly different from the D-gal-vehicle group). The *bars* indicate the SE

In the present study, we also observed a transcription factor CREB in the hippocampus because CREB is critical for consolidation of long-term memory [41, 42] and long-lasting long-term potentiation [43–46]. pCREB immunoreactivity was significantly decreased in the D-gal-vehicle group compared to that in the control group. This result is supported by previous studies that a specific and temporally controlled inhibition of CREB function disrupted performance in various forms of the hippocampus [47–50]. However, in the present study, we found that the administration of Pyr in combination with SB significantly increased the water maze performance and pCREB immunoreactivity in the hippocampus.

In conclusion, our findings indicate that treatment with Pyr in combination with SB distinctively restored age-related reductions in memory function, cell proliferation, neuroblast differentiation, pCREB immunoreactivity in the dentate gyrus of a mouse model of aging induced by D-gal, and we suggest that these drugs may be helpful in ameliorating age-related memory deficits.

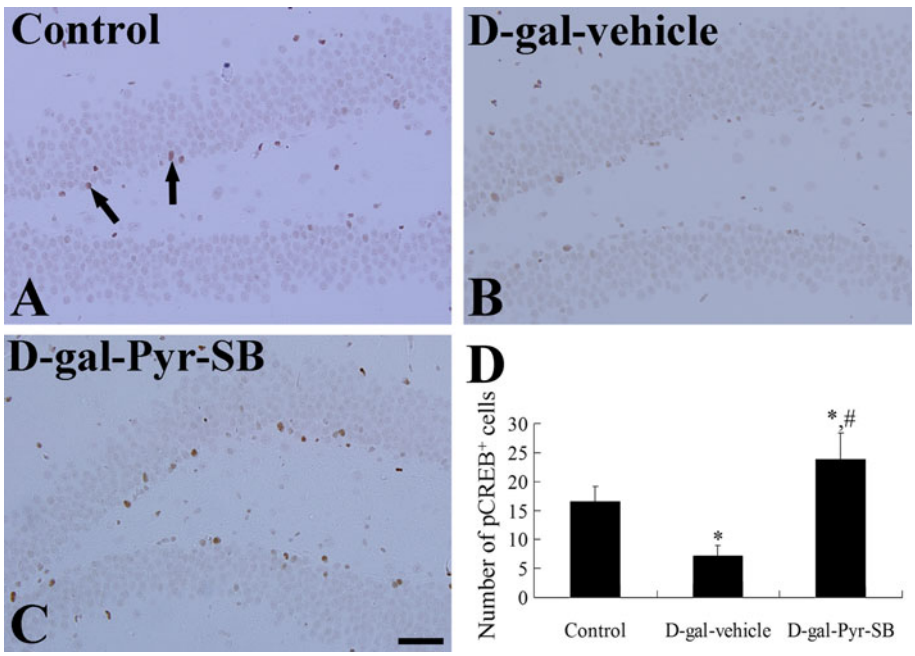

Fig. 6 Immunohistochemistry for pCREB in the dentate gyrus of the control (**a**), D-gal-vehicle (**b**), and D-gal-Pyr-SB (**c**) groups. pCREB-positive nuclei (*arrows*) are mainly detected in the subgranular zone of the dentate gyrus. pCREB-positive nuclei are significantly decreased in the D-gal-vehicle group, and they are increased in the D-gal-Pyr-SB group compared to those in the D-gal-vehicle group. GCL, granule cell layer; *ML* molecular layer, *PL* polymorphic layer. *Scale bar* = 50 μm. **d** The mean number of pCREB-positive nuclei per section in the dentate gyrus of all groups ($n = 7$ per group; $^{*}P < 0.05$, indicating a significant difference compared to the control group; $^{\#}P < 0.05$, significantly different from the D-gal-vehicle group). The *bars* indicate the SEM

Acknowledgments The authors would like to thank Mr. Seung Uk Lee and Mrs. Hyun Sook Kim for their technical help in this study. This work was supported by the National Research Foundation of Korea Grant funded by the Korean Government (MEST), Republic of Korea (2010-0007711).

References

1. Srivastava N, Seth K, Srivastava N, Khanna VK, Agrawal AK (2008) Functional restoration using basic fibroblast growth factor (bFGF) infusion in Kainic acid induced cognitive dysfunction in rat: neurobehavioural and neurochemical studies. Neurochem Res 33:1169–1177
2. Goodman T, Trouche S, Massou I et al (2010) Young hippocampal neurons are critical for recent and remote spatial memory in adult mice. Neuroscience 171:769–778
3. Koehl M, Abrous DN (2011) A new chapter in the field of memory: adult hippocampal neurogenesis. Eur J Neurosci 33: 1101–1114
4. Heine VM, Maslam S, Joëls M, Lucassen PJ (2004) Prominent decline of newborn cell proliferation, differentiation, and apoptosis in the aging dentate gyrus, in absence of an age-related hypothalamus-pituitary-adrenal axis activation. Neurobiol Aging 25:361–375
5. Hwang IK, Yoo KY, Li H et al (2007) Differences in doublecortin immunoreactivity and protein levels in the hippocampal dentate gyrus between adult and aged dogs. Neurochem Res 32:1604–1609
6. Hwang IK, Yoo KY, Yi SS et al (2008) Age-related differentiation in newly generated DCX immunoreactive neurons in the subgranular zone of the gerbil dentate gyrus. Neurochem Res 33: 867–872
7. Kuhn HG, Dickinson-Anson H, Gage F (1996) Neurogenesis in the dentate gyrus of the adult rat: age-related decrease of neuronal progenitor proliferation. J Neurosci 16:2027–2033
8. Rao MS, Hattiangady B, Shetty AK (2006) The window and mechanisms of major age-related decline in the production of new neurons within the dentate gyrus of the hippocampus. Aging Cell 5:545–558
9. Seki T, Arai Y (1995) Age-related production of new granule cells in the adult dentate gyrus. Neuroreport 6:2479–2482
10. Chiu CS, Deng JS, Hsieh MT et al (2009) Yam (*Dioscorea pseudojaponica* Yamamoto) ameliorates cognition deficit and attenuates oxidative damage in senescent mice induced by D-galactose. Am J Chin Med 37:889–902
11. Luo Y, Niu F, Sun Z et al (2009) Altered expression of Aβ metabolism-associated molecules from D-galactose/$AlCl_3$ induced mouse brain. Mech Ageing Dev 130:248–252
12. Tian J, Ishibashi K, Ishibashi K et al (2005) Advanced glycation endproduct-induced aging of the retinal pigment epithelium and choroid: a comprehensive transcriptional response. Proc Natl Acad Sci USA 102:11846–11851
13. Zhong SZ, Ge QH, Qu R, Li Q, Ma SP (2009) Paeonol attenuates neurotoxicity and ameliorates cognitive impairment induced by D-galactose in ICR mice. J Neurol Sci 277:58–64
14. Shen YX, Xu SY, Wei W et al (2002) Melatonin reduces memory changes and neural oxidative damage in mice treated with D-galactose. J Pineal Res 32:173–178
15. Wei H, Li L, Song Q, Ai H, Chu J, Li W (2005) Behavioural study of the D-galactose induced aging model in C57BL/6 J mice. Behav Brain Res 157:245–251
16. Xu XH, Zhao TQ (2002) Effects of puerarin on D-galactose-induced memory deficits in mice. Acta Pharmacol Sin 23: 587–590
17. Cui X, Zuo P, Zhang Q et al (2006) Chronic systemic D-galactose exposure induces memory loss, neurodegeneration, and oxidative damage in mice: protective effects of R-α-lipoic acid. J Neurosci Res 84:647–654
18. Hsieh HM, Wu WM, Hu ML (2009) Soy isoflavones attenuate oxidative stress and improve parameters related to aging and Alzheimer's disease in C57BL/6 J mice treated with D-galactose. Food Chem Toxicol 47:625–632
19. Zhang Q, Huang Y, Li X, Cui X, Zuo P, Li J (2005) GM1 ganglioside prevented the decline of hippocampal neurogenesis associated with D-galactose. Neuroreport 16:1297–1301
20. Zhang Q, Li X, Cui X, Zuo P (2005) D-Galactose injured neurogenesis in the hippocampus of adult mice. Neurol Res 27: 552–556
21. Song X, Bao M, Li D, Li YM (1999) Advanced glycation in D-galactose induced mouse aging model. Mech. Ageing Dev 108: 239–251
22. Alarcón JM, Malleret G, Touzani K et al (2004) Chromatin acetylation, memory, and LTP are impaired in $CBP^{+/-}$ mice: a model for the cognitive deficit in Rubinstein-Taybi syndrome and its amelioration. Neuron 42:947–959
23. Lattal KM, Barrett RM, Wood MA (2007) Systemic or intrahippocampal delivery of histone deacetylase inhibitors facilitates fear extinction. Behav Neurosci 121:1125–1131
24. Levenson JM, O'Riordan KJ, Brown KD, Trinh MA, Molfese DL, Sweatt JD (2004) Regulation of histone acetylation during memory formation in the hippocampus. J Biol Chem 279: 40545–40559
25. Dokmanovic M, Marks PA (2005) Prospects: histone deacetylase inhibitors. J Cell Biochem 96:293–304
26. Yoo DY, Kim W, Kim DW et al (2011) Pyridoxine enhances cell proliferation and neuroblast differentiation by upregulating the GABAergic system in the mouse dentate gyrus. Neurochem Res 36:713–721
27. Yoo DY, Kim W, Nam SM et al (2011) Synergistic effects of sodium butyrate, a histone deacetylase inhibitor, on increase of neurogenesis induced by pyridoxine and increase of neural proliferation in the mouse dentate gyrus. Neurochem Res 36: 1850–1857
28. Brown JP, Couillard-Després S, Cooper-Kuhn CM, Winkler J, Aigner L, Kuhn HG (2003) Transient expression of doublecortin during adult neurogenesis. J Comp Neurol 467:1–10
29. Couillard-Despres S, Winner B, Schaubeck S et al (2005) Doulecortin expression levels in adult brain reflect neurogenesis. Eur J Neurosci 21:1–14
30. Franklin KBJ, Paxinos G (1997) The mouse brain in stereotaxic coordinates. Academic Press, San Diego
31. Wei H, Cai Y, Chu J, Li C, Li L (2008) Temporal gene expression profile in hippocampus of mice treated with D-galactose. Cell Mol Neurobiol 28:781–794
32. Kumar A, Prakash A, Dogra S (2010) Naringin alleviates cognitive impairment, mitochondrial dysfunction and oxidative stress induced by D-galactose in mice. Food Chem Toxicol 48:626–632
33. Kilgore M, Miller CA, Fass DM et al (2010) Inhibitors of class 1 histone deacetylases reverse contextual memory deficits in a mouse model of Alzheimer's disease. Neuropsychopharmacology 35:870–880
34. Riggs KM, Spiro A 3rd, Tucker K, Rush D (1996) Relations of vitamin B-12, vitamin B-6, folate, and homocysteine to cognitive performance in the Normative Aging Study. Am J Clin Nutr 63: 306–314
35. Eriksson PS, Perfilieva E, Björk-Eriksson T et al (1998) Neurogenesis in the adult human hippocampus. Nat Med 4:1313–1317
36. Dakshinamurti K, Paulose CS, Viswanathan M, Siow YL, Sharma SK, Bolster B (1990) Neurobiology of pyridoxine. Ann N Y Acad Sci 585:128–144

37. Kirksey A, Morré DM, Wasynczuk AZ (1990) Neuronal development in vitamin B_6 deficiency. Ann N Y Acad Sci 585:202–218
38. Guan JS, Haggarty SJ, Giacometti E et al (2009) HDAC2 negatively regulates memory formation and synaptic plasticity. Nature 459:55–60
39. Vecsey CG, Hawk JD, Lattal KM et al (2007) Histone deacetylase inhibitors enhance memory and synaptic plasticity via CREB:CBP-dependent transcriptional activation. J Neurosci 27:6128–6140
40. Wood MA, Attner MA, Oliveira AM, Brindle PK, Abel T (2006) A transcription factor-binding domain of the coactivator CBP is essential for long-term memory and the expression of specific target genes. Learn Mem 13:609–617
41. Izquierdo LA, Barros DM, Vianna MR et al (2002) Molecular pharmacological dissection of short-and long-term memory. Cell Mol Neurobiol 22:269–287
42. Silva AJ, Kogan JH, Frankland PW, Kida S (1998) CREB and memory. Annu Rev Neurosci 21:127–148
43. Bourtchuladze R, Frenguelli B, Blendy J, Cioffi D, Schutz G, Silva AJ (1994) Deficient long-term memory in mice with a targeted mutation of the cAMP-responsive element-binding protein. Cell 79:59–68
44. Impey S, Mark M, Villacres EC, Poser S, Chavkin C, Storm DR (1996) Induction of CRE-mediated gene expression by stimuli that generate long-lasting LTP in area CA1 of the hippocampus. Neuron 16:973–982
45. Mizuno M, Yamada K, Maekawa N, Saito K, Seishima M, Nabeshima T (2002) CREB phosphorylation as a molecular marker of memory processing in the hippocampus for spatial learning. Behav Brain Res 133:135–141
46. Schulz S, Siemer H, Krug M, Höllt V (1999) Direct evidence for biphasic cAMP responsive element-binding protein phosphorylation during long-term potentiation in the rat dentate gyrus in vivo. J Neurosci 19:5683–5692
47. Florian C, Mons N, Roullet P (2006) CREB antisense oligodeoxynucleotide administration into the dorsal hippocampal CA3 region impairs long- but not short-term spatial memory in mice. Learn Mem 13:465–472
48. Guzowski JF, McGaugh JL (1997) Antisense oligodeoxynucleotide-mediated disruption of hippocampal cAMP response element binding protein levels impairs consolidation of memory for water maze training. Proc Natl Acad Sci USA 94:2693–2698
49. Huang YY, Pittenger C, Kandel ER (2004) A form of long-lasting, learning-related synaptic plasticity in the hippocampus induced by heterosynaptic low-frequency pairing. Proc Natl Acad Sci USA 101:859–864
50. Pittenger C, Huang YY, Paletzki RF et al (2002) Reversible inhibition of CREB/ATF transcription factors in region CA1 of the dorsal hippocampus disrupts hippocampus-dependent spatial memory. Neuron 34:447–462